# Layer-by-Layer Self-Assembled Pyrrole-Based Donor−Acceptor Chromophores as Electro-Optic Materials

Antonio Facchetti,*[,†,⊥] Alessandro Abbotto,[†] Luca Beverina,[†] Milko E. van der Boom,[‖] Pulak Dutta,[§] Guennadi Evmenenko,[§] Giorgo A. Pagani,[†] and Tobin J. Marks*[,‡]

*Department of Material Science, University of Milano−Bicocca, via Cozzi 53, 20125 Milano, Italy, Departments of Chemistry and Physics and Astronomy, and the Materials Research Center, Northwestern University, Evanston, Illinois 60208-3113, and Department of Organic Chemistry, The Weizmann Institute of Science, Rehovot, 76100, Israel*

*Received September 9, 2002. Revised Manuscript Received January 10, 2003*

The synthesis of the heterocycle-based diethanolaminomethyl-functionalized derivative 1-(pyridin-4-yl)-2-[(*N*-methylpyrrol-2-yl)-5-methylenediethanolamine]ethene (**2**) from (1-pyridin-4-yl)-2-(*N*-methyl-pyrrol-2-yl)ethene (**1**) and their methylpyridinium dyes 1-(*N*-methylpyridinio)-2-[(*N*-methylpyrrol-2-yl)-5-methylenediethanolamine]ethene iodide (**3**) and 1-(*N*-methylpyridinio)-2-[(*N*-methylpyrrol-2-yl)-5-methylenediethanolamine]ethene iodide (**4**) is described. NLO-active chromophore monolayers **SA-1** and **SA-2** were obtained by reaction of *p*-iodomethylphenyldiiodochlorosilane (**5**)-functionalized substrates and dye precursors **1** and **2**, respectively. A $\chi^{(2)}$ value of ∼120 pm/V is observed for **SA-2**. The new diethanolaminomethyl-functionalized chromophore **2** is also a suitable building block for the layer-by-layer formation of intrinsically acentric, highly transparent nonlinear optical/electro-optic multilayers (SAS = self-assembled superlattice). The organic SAS films are characterized by a combination of physicochemical methods including synchrotron specular X-ray reflectivity, angle-dependent polarized second-harmonic generation, optical (absorption and photoluminescence) spectroscopy, X-ray photospectroscopy, atomic force microscopy, and advancing contact angle measurements.

## Introduction

Design of molecule-based photonic materials and development of "all-organic" electro-optic (EO) devices may greatly enhance optical network speed, capacity, and bandwidth for data networking and telecommunications.[1] Among the various approaches to preparing suitable EO materials,[2−11] layer-by-layer molecular self-assembly (SA), and templated formation of intrinsically polar arrays of high-$\beta$ chromophores, grown directly on silicon or related substrates, is attractive in that it requires neither electric field poling, poling electrodes, nor electrically matched buffer layers.[6−11] We demonstrated recently that intrinsically acentric superlattices (SASs = self-assembled superlattices) prepared by wet chemical self-assembly allow ready device integration and significantly reduce device design complexity.[12,13] A wide range of push−pull/donor−acceptor chromophores have been incorporated into poled-polymer and Lang-

* Corresponding authors. E-mail: a-facchetti@northwestern.edu; t-marks@northwestern.edu.
† University of Milano−Bicocca.
‡ Department of Chemistry and the Materials Research Center, Northwestern University.
§ Department of Physics and Astronomy and the Materials Research Center, Northwestern University.
‖ The Weizmann Institute of Science.
⊥ Current address: Department of Chemistry and the Materials Research Center, Northwestern University.

(1) For reviews: (a) van der Boom, M. E. *Angew. Chem., Int. Ed.* **2002**, *18*, 3363−3366. (b) Würthner, F.; Wortmann, R.; Meerholz, K. *ChemPhysChem* **2002**, *3*, 17−31. (c) Samijn, C.; Verbiest, T. Persoons, A. *Macromol. Rapid Commun.* **2000**, *21*, 1−15. (d) Dalton, L. R.; Steier, W. H.; Robinson, B. H.; Zhang, C.; Ren, A.; Garner, S.; Chen, A.; Londergan, T.; Irwin, L.; Carlson, B.; Fifield, L.; Phelan, G.; Kincaid, C.; Amend, J.; Jen, A. *J. Mater. Chem.* **1999**, *9*, 1905−1920. (e) Saadeh, H.; Yu. D.; Wang, L. M.; Yu, L. P. *J. Mater. Chem.* **1999**, *9*, 1865−1873. (f) Robinson, B. H.; Dalton, L. R.; Harper, A. W.; Ren, A.; Wang, F.; Zhang, C.; Todorova, G.; Lee, M.; Aniszfeld, R.; Garner, S.; Chen, A.; Steier, W. H.; Houbrecht, S.; Persoons, A.; Ledoux, I.; Zyss, J.; Jen, A. K. Y. *Chem. Phys.* **1999**, *245*, 487−506. (g) Marder, S. R.; Kippelen, B.; Jen, A. K. Y.; Peyghambarian, N. *Nature* **1997**, *388*, 845−851. (h) Long, N. J. *Angew. Chem., Int. Ed. Engl.* **1995**, *34*, 21−38. (i) *Chem. Rev.* (Special Issue on Optical Nonlinearities in Chemistry, Ed.: D. M. Burland) **1994**, *94*, 1−278. (j) *Molecular Nonlinear Optics−Materials, Physics and Devices*; Zyss, J., Ed.; Academic Press: San Diego, CA, 1994.

(2) (a) Ma, H.; Chen, B. Q.; Sassa, T. A.; Dalton, L. R., Jen, A. K.-Y. *J. Am. Chem. Soc.* **2001**, *123*, 986−987. (b) Wang, C. Zhang, C.; Lee, M. S.; Dalton, L. R.; Zhang, H.; Steier, W. H. *Macromolecules* **2001**, *34*, 2359−2363. (c) Hayden, L. M.; Kim, W.-K.; Chafin, A. P.; Lindsay, G. A. *Macromolecules* **2001**, *34*, 1493−1495. (d) Samijn, C.; Verbiest, T.; Persoons, A. *Macromol. Rapid Commun.* **2000**, *21*, 1−15. (e) Jiang, H.; Kakkar, A. K. *J. Am. Chem. Soc.* **1999**, *121*, 3657−3665. (f) Yitzchaik, S.; Di Bella, S.; Lundquist, P. M.; Wong, G. K.; Marks, T. J. *J. Am. Chem. Soc.* **1997**, *119*, 2995−3002.

(3) (a) Lemaître, N.; Attias, A. J.; Ledoux, I.; Zyss, J. *Chem. Mater.* **2001**, *13*, 1420−1427. (b) Würthner, F.; Yao, S.; Schilling, J.; Wortmann, R.; Redi-Abshiro, M.; Mecher, E.; Gallego-Gomez, F.; Meerholz, K. *J. Am. Chem. Soc.* **2001**, *123*, 2810−2824. (c) RekaO, E. D.; Baudin, J.-B.; Jullien, L.; Ledoux, I.; Zyss, J.; Blanchard-Desce, M. *Chem. Eur. J.* **2001**, *7*, 4395−4402. (d) Schwartz, H.; Mazor, R.; Khodorkovsky, V.; Shapiro, L.; Klug, J. T.; Kovalev, E.; Meshulam, G.; Berkovic, G.; Kotler, Z.; Efrima, S. *J. Phys. Chem. B* **2001**, *105*, 5914−5921. (e) Roberts, M. J.; Lindsay, G. A.; Herman, W. N.; Wynne, K. J. *J. Am. Chem. Soc.* **1998**, *120*, 11202−11203. (f) Ahlheim, M.; Barzoukas, M.; Bedworth, P. V.; Blanchard-Desce, M.; Fort,.; Hu, Z.-Y.; Marder, S. R.; Perry, J. W.; Runser, C.; Staehelin, M.; Zysset, B. *Science* **1996**, *271*, 335−337. (g) Wijekoon, W. M. K. P.; Wijayu, S. K.; Bhawalkar, J. D.; Prasad, P. N.; Penner, T. L.; Armstrong, N. J.; Ezenyilimba, M. C.; Williams, D. J. *J. Am. Chem. Soc.* **1996**, *118*, 4480−4483. (h) Ashwell, G. J.; Jackson, P. D.; Crossland, W. A. *Nature* **1994**, *368*, 438−440.

10.1021/cm020929d CCC: $25.00 
Published on Web 02/14/2003

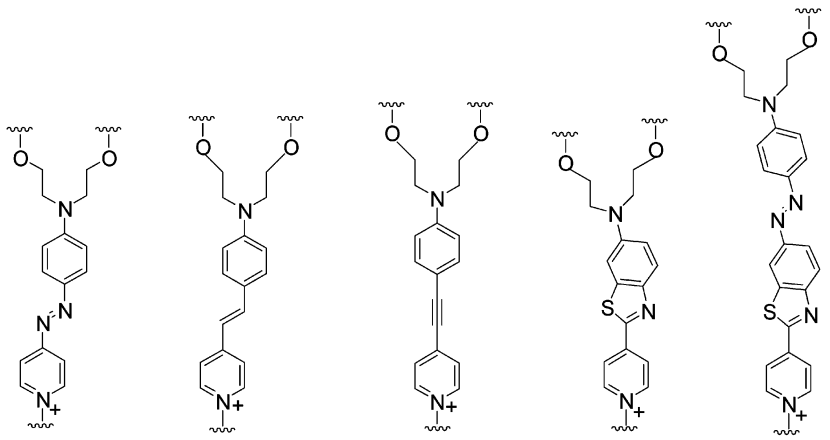

**Figure 1.** High-$\beta$ push−pull chromophore building blocks used for layer-by-layer formation of acentric siloxane-based self-assembled superlattices.[10,11]

muir−Blodgett based films.[2−4] Hitherto, covalently bound siloxane-based EO multilayer films have exclusively utilized pyridinium acceptor and aminophenyl donor push−pull chromophores as building blocks (Figure 1).[10,11]

To date, however, no studies have reported implementing in the SAS strategy building blocks having both $\pi$-deficient and $\pi$-excessive heterocycles as sole donor and acceptor units.[14]

In a recent series of papers,[9,15] some of us reported the systematic exploration of heterocycles as key components in push−pull chromophores for second- and third-order NLO phenomena. In addition, we very recently described[16] the preparation of acentric, highly transparent azinium−pyrrole monolayers on silicon and glass. In this contribution, we report the straightforward and high-yield synthesis of the diethanolaminomethyl-functionalized chromophore system **2** and of the corresponding methoiodide salts **3** and **4**, starting from the basic pyridine−(C═C)−pyrrole skeleton **1** (Figure 2).

As judged from the second-harmonic generation measurements, the response of a SA monolayer of chromophore **1** (**SA-1**) is the highest among the azine heterocycle systems investigated, reaching a $\chi^{(2)}$ value of ∼140 pm/V ($\lambda_0$ = 1064 nm).[16] We demonstrate here that proper chemical modification of **1** to give **2** allows the preparation of *multilayer assemblies* using an iterative three-step reaction sequence involving the following:[11] (i) covalent chemisorption of an alkyl-halide-functionalized silyl coupling agent **5** to a hydroxylated substrate surface, (ii) quaternization of the chromophore

(4) (a) Ricceri, R.; Abbotto, A.; Facchetti, A.; Grando, D.; Gabrielli, G.; Pagani, G. A. *Colloids Surf., A* **1999**, *150*, 289−296. (b) Ricceri, R.; Neto, C.; Abbotto, A.; Facchetti, A.; Pagani, G. A. *Langmuir* **1999**, *15*, 2149−2151. (c) Ricceri, R.; Abbotto, A.; Facchetti, A.; Pagani, G. A.; Gabrielli, G. *Thin Solid Films* **1999**, 340, 218−230. (d) Ricceri, R.; Grando, D.; Abbotto, A.; Facchetti, A.; Pagani, G. A.; Gabrielli, G. *Langmuir* **1997**, *13*, 5787−5790. (e) Ricceri, R.; Abbotto, A.; Facchetti, A.; Pagani, G. A.; Gabrielli, G. *Langmuir* **1997**, *13*, 4182−4184. (f) Ricceri, R.; Abbotto, A.; Facchetti, A.; Pagani, G. A.; Gabrielli, G. *Langmuir* **1997**, *13*, 3434−3437.

(5) (a) Evans, O. R.; Lin, W. *Chem. Mater.* **2001**, *13*, 3009−3017. (b) Kanazawa, A.; Ikeda, T.; Abe, J. *Angew. Chem., Int. Ed.* **2000**, *39*, 612−615. (c) Coe, B. J. *Chem. Eur. J.* **1999**, *5*, 2464−2471. (d) Lin, W.; Wang, Z.; Ma, L. *J. Am. Chem. Soc.* **1999**, *121*, 11249−11250. (e) Johal, M. S.; Cao, Y. W.; Chai, X. D.; Smilowitz, L.B.; Robinson, J. M.; Li, T. J. McBranch, D.; Li, D.-Q. *Chem. Mater.* **1999**, *11*, 1962−1965. (f) Lin, W.; Evans, O. R.; Xiong, R.-G.; Wang, Z. *J. Am. Chem. Soc.* **1998**, *120*, 13272−13273. (g) Di Bella, S.; Fragalà, I.; Ledoux, I.; Diaz-Garcia, M. A.; Marks T. J. *J. Am. Chem. Soc.* **1997**, *119*, 9550−9557.

(6) (a) Bakiamoh, S. B.; Blanchard, G. J. *Langmuir* **2001**, *17*, 3438−3446. (b) Neff, G. A.; Helfrich, M. R.; Clifton, M. C.; Page, C. J. *Chem. Mater.* **2000**, *12*, 2363−2371. (c) Flory, W. C.; Mehrens, S. M.; Blanchard, G. J. *J. Am. Chem. Soc.* **2000**, *122*, 7976−7985. (d) Hanken, D. G.; Naujok, R. R.; Gray, J. M.; Corn, R. M. *Anal. Chem.* **1997**, *69*, 240−248. (e) Katz, H. E.; Wilson, W. L.; Scheller, G. *J. Am. Chem. Soc.* **1994**, *116*, 6636−6640. Examples of metal-ion-based centrosymmetric layer-by-layer SA: (f) Doron-Mor, H.; Hatzor, A.; Vaskevich, A.; van der Boom-Moav, T.; Shanzer, A.; Rubinstein I.; Cohen, H. A. *Nature* **2000**, *406*, 382−385. (g) Fang, M.; Kaschak, D. M.; Sutorik, A. C.; Mallouk, T. E. *J. Am. Chem. Soc.* **1997**, *119*, 12184−12191.

(7) Acentric hydrogen-bonded silane−$Cu^{2+}$ superlattices: (a) Maoz, R.; Yam, R.; Berkovic, G.; Sagiv, J. In *Thin Films*; Ulman, A., Ed.; Academic Press: San Diego, CA, 1995; Vol. 20, pp 41−66.

(8) (a) Van Cott, K. E.; Guzy, M.; Neyman, P.; Brands, C.; Heflin, J. R.; Gibson, H. W.; Davis, R. M. *Angew. Chem., Int. Ed.* **2002**, *17*, 3226−3228. (b) Huang, W.; Helvenston, M.; Casson, J. L.; Wang, R.; Bardeau, J.-F.; Lee, Y.; Johal, M. S.; Swanson, B. I.; Robinson, J. M.; Li, D.-Q. *Langmuir* **1999**, *15*, 6510−6514. (c) Li, D.-Q.; Swanson, B. I.; Robinson, J. M.; Hoffbauer, M. A. *J. Am. Chem. Soc.* **1993**, *115*, 6975−6980.

(9) (a) Facchetti, A.; van der Boom, M. E.; Abbotto, A.; Beverina, L.; Marks, T. J.; Pagani, G. A. *Langmuir* **2001**, *17*, 5939−5942. (b) Pagani, G. A.; Abbotto, A.; Beverina, L.; Bradamante, S.; Facchetti, A.; van der Boom, M. E.; Marks, T. J. *Polym. Prepr.* **2001**, *42*, 567−568.

(10) (a) van der Boom, M. E.; Evmenenko, G.; Dutta, P.; Marks, T. J. *Langmuir* **2002**, *18*, 3704−3707. (b) van der Boom, M. E.; Evmenenko, G.; Dutta, P.; Marks, T. J. *Polym. Mater. Sci. Eng.* **2002**, *87*, 375−376. (c) van der Boom, M. E.; Evmenenko, G.; Dutta, P.; Marks, T. J. *Adv. Funct. Mater.* **2001**, *11*, 393−397. (d) Evmenenko, G.; van der Boom, M. E.; Kmetko, J.; Dugan, S. W.; Marks, T. J.; Dutta, P. *J. Chem. Phys.* **2001**, *115*, 6722−6727. (e) Zhu, P.; van der Boom, M. E.; Evmenenko, G.; Dutta, P.; Marks, T. J. *Polym. Prepr.* **2001**, *42*, 579−580. (f) van der Boom, M. E.; Richter, A. G.; Malinsky, J. E.; Dutta, P.; Marks, T. J. *Chem. Mater.* **2001**, *13*, 15−17. (g) van der Boom, M. E.; Richter, A. G.; Malinsky, J. E.; Dutta, P.; Marks, T. J.; Lee, P. A.; Armstrong, N. R. *Polym. Mater. Sci. Eng.* **2000**, *83*, 160−161. (h) van der Boom, M. E.; Richter, A. G.; Malinsky; J. E.; Dutta, P.; Marks, T. J. *NSLS Activity Report; Science Highlights*; Corwin, M. A., Ehrlich, S. N., Eds.; Brookhaven Science Associates, Inc.: Upton, NY, 1999; Vol. 2, pp 47−49. (i) Zhu, P.; van der Boom, M. E.; Kang, H.; Evmenenko, G.; Dutta, P.; Marks, T. J. *Chem. Mater.* **2002**, *14*, 4982−4989.

(11) (a) Lin, W.; Lee, T.-L.; Lyman, P. F.; Lee, J.; Bedzyk, M. J.; Marks, T. J. *J. Am. Chem. Soc.* **1997**, *119*, 2205−2211. (b) Lin, W.; Lin, W.; Wong, G. K.; Marks, T. J. *J. Am. Chem. Soc.* **1996**, *118*, 8034−8042. (c) Yitzchaik, S.; Marks, T. J. *Acc. Chem. Res.* **1996**, *29*, 197−202. (d) Marks, T. J.; Ratner, M. *Angew. Chem., Int. Ed. Engl.* **1995**, *34*, 155−173. (e) Lin, W.; Yitzchaik, S.; Lin, W.; Malik, A.; Durbin, M. K.; Richter, A. G.; Wong, G. K.; Dutta, P.; Marks, T. J. *Angew. Chem., Int. Ed. Engl.* **1995**, *34*, 1497−1499. (f) Li, D.-Q.; Ratner, M. A.; Marks, T. J. *J. Am. Chem. Soc.* **1990**, *112*, 7389−7390.

(12) Poled-polymer modulators are rapidly approaching or even exceeding the performance of commercially available inorganic EO devices. See: (a) Zhang, H.; Oh, M.-C.; Szep, A.; Steier, W. H.; Zhang, C.; Dalton, L. R. *Appl. Phys. Lett.* **2001**, *78*, 3136−3138. (b) Lee, S.-S.; Garner, S. M.; Chuyanov, V.; Zhang, H.; Steier, W. H.; Wang, F.; Dalton, L. R.; Udupa, A. H.; Fetterman, H. R. *IEEE J. Quantum Electron.* **2000**, *36*, 527−532. (c) Shi, Y.; Zhang, C.; Zhang, H.; Bechtel, J. H.; Dalton, L. R.; Robinson, B. H.; Steier, W. H. *Science* **2000**, *288*, 119−122. (d) For a recent review, see: Dalton, L. R. *Opt. Eng.* **2000**, *39*, 589−595.

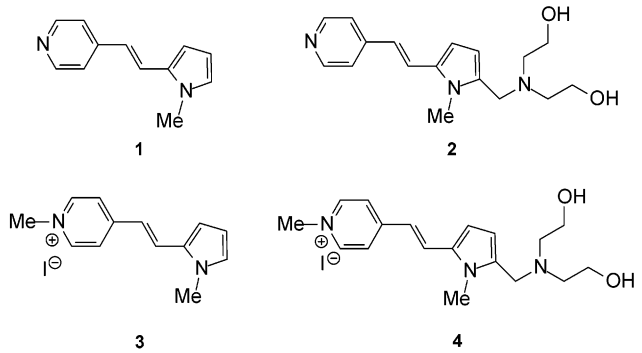


**Figure 2.** Chromophore precursors **1** and **2** and the corresponding methoiodide salts **3** and **4**.

precursor by the covalently bound coupling layer to generate an EO-active coupling/chromophore bilayer, and (iii) reaction of the chromophoric diethanolamine surface **SA-2** with octachlorotrisiloxane (**6**) to form a trilayer (Figure 3). This latter "capping" step deposits a robust polysiloxane film, generates a large density of reactive hydroxyl sites necessary for subsequent coupling layer (**5**) deposition, and provides structural stabilization via interchromophore cross-linking.[10,11,17]

## Experimental Section

**General Procedures.** All reactions were carried out under an inert atmosphere. Solvents were dried over Na/K alloy, distilled, and degassed before use. The reagent *p*-(iodomethyl)-phenyldiiodochlorosilane (**5**) was synthesized according to procedures described elsewhere.[8b] Silicon(111) substrates and octachlorotrisiloxane (**6**) were purchased from Semiconductor Processing, Inc. and Gelest, Inc., respectively. Sodium lime glass slides and Si(111) wafers ($1 \times 1$ cm$^2$) were cleaned by immersion in a "piranha" solution ($H_2SO_4$:30% $H_2O_2$ = 70:30 v/v) at 80 °C for 1 h. (Warning: *piranha solution is an extremely strong oxidation reagent*.) Subsequently, the substrates were rinsed repeatedly with deionized (DI) water and then sonicated in a solution of DI $H_2O$, 30% $H_2O_2$, and $NH_3$ (5:1:1 v/v/v) for 45 min. The substrates were then washed with copious amounts of DI $H_2O$ and dried at 115 °C overnight before deposition of coupling agent **5**. Samples were stored in the dark. Aqueous contact angles were measured on a standard tensiometric bench instrument fitted with a Teflon micrometer syringe (Gilmont Instruments, Inc.). Polarized second-harmonic generation measurements were made in the transmission mode by placing the glass slides in the path of the 1.06-$\mu$m output of a Q-switched p-polarized light from a Nd:YAG laser. The details of this setup can be found elsewhere.[18] $^1$H NMR spectra were recorded on a Varian Gemini 300 and Bruker AMX-500 instrument using the residual proton signal of the deuterated solvents as an internal standard. UV−vis spectra were recorded with a Varian Cary 1E spectrophotometer. Synchrotron X-ray reflectivity studies were performed at beamline X23B using a Huber four-circle diffractometer in the specular reflection mode (e.g., incident angle is equal to exit angle). X-rays of energy $E = 9.653$ keV ($\lambda = 1.284$ Å) were used for all measurements. The beam size was 0.35 mm vertically and 2.0 mm horizontally. The samples were placed under helium during the measurements to reduce the background scattering from the ambient atmosphere and radiation damage. The experiments were performed at room temperature. The off-specular background was measured and subtracted from the specular counts.

**Synthesis of 1-(Pyrid-4-yl)-2-(*N*-methylpyrrol-2-yl)-ethene (1).** This system was prepared with slight modification of our previous procedure.[15c] Under a $N_2$ atmosphere, a solution of 4-picoline (1.16 g, 12.5 mmol) in anhydrous DMF (6 mL) was added to a suspension of sodium hydride (60% dispersion in mineral oil, 12.5 mmol) in the same solvent (14 mL). After the solution was stirred for 2 h at 60 °C, a solution of *N*-methylpyrrole-2-carboxyaldehyde (1.35 g, 12.4 mmol) in anhydrous DMF (8 mL) was then added to the solution of the

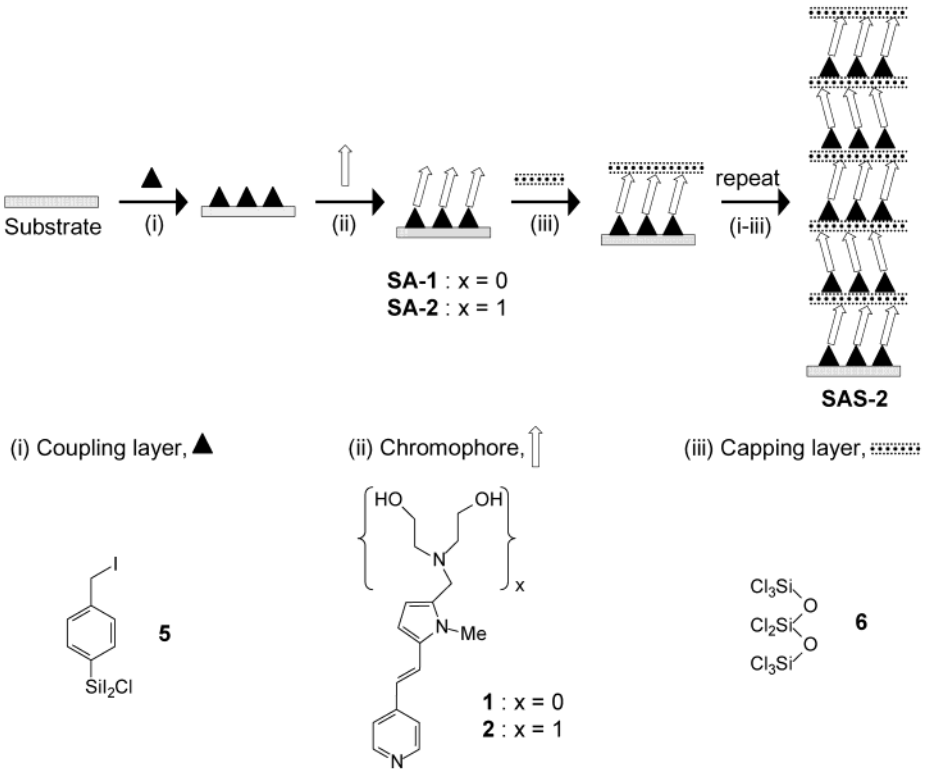


**Figure 3.** Assembly of chromophoric superlattices by an iterative sequence of (i) covalent chemisorption of (*p*-iodomethyl)-phenyldiiodochlorosilane (**5**) onto hydrophilic substrates to form a "coupling" layer, (ii) spin-coating of a methanol solution of chromophore precursor **1** or **2** (20 mM; 2000 rpm) followed by vacuum oven treatment (20 min/105 °C/30 mmHg; static vacuum), and (iii) reaction of the quaternized chromophore **2**-based monolayer with octachlorotrisiloxane (**6**).

anion. After this solution was stirred for 7 h at 60 °C, the reaction mixture was poured onto ice (80 mL) to give a yellow solid, which was collected by filtration to afford the pure material after sublimation (1.38 g, 7.50 mmol, 60.6%): mp 132 °C (lit.[15c] 126−127 °C). $^1$H NMR ($CDCl_3$): $\delta$ 8.51 (2 H, d, $^3J$ = 3.6), 7.26 (2 H, d), 7.16 (1 H, d, $^3J$ = 16.1), 6.74 (1 H, d), 6.67 (1 H, dd, $^3J$ = 2.0), 6.56 (1H, dd, $^3J$ = 1.7), 6.16 (1 H, dd, $^3J$ = 2.7), 3.71 (3 H, s).

**Synthesis of 1-(*N*-Methyl-4-pyridinio)-2-(*N*-methylpyrrol-2-yl)ethene Iodide (3).** Methyl iodide (0.23 g, 1.60 mmol) was added to a solution of 1-(pyrid-4-yl)-2-(*N*-methylpyrrol-2-yl)ethene (**1**) (0.15 g, 0.81 mmol) in dry toluene (8 mL). After the solution was stirred overnight at room temperature, a precipitate formed and was collected and washed several times with toluene. The orange solid was dried at 80 °C under vacuum and found to be the pure title compound (0.22 g, 0.67 mmol, 82.7% yield): mp 254 °C (*i*-PrOH−$H_2O$). $^1$H NMR (DMSO-$d_6$): $\delta$ 7.36 (1H, d, $^3J$ = 3.8), 8.63 (2H, d, $^3J$ = 6.6), 8.04 (2H, d), 7.85 (1H, d, $^3J$ = 16.0), 7.03 (1H, d, $^3J$ = 3.1), 7.01 (1H, d), 7.83 (1H, d, $^3J$ = 3.7), 6.16 (1H, dd), 4.12 (3 H, s), 3.75 (3 H, s). Anal. Calcd for $C_{13}H_{15}IN_2$: C, 47.87; H, 6.64; N, 8.59. Found: C, 47.90; H, 4.68; N, 8.49.

**Synthesis of 1-(Pyrid-4-yl)-2-[(*N*-methylpyrrol-2-yl)-5-methylenediethanolamine]ethene (2).** Under $N_2$, a mixture of **1** (2.00 g, 10.9 mmol), *p*-toluenesulfonic acid (1.89 g, 11 mmol), *p*-formaldehyde (0.66 g, 22 mmol), and diethanolamine (3.47 g, 33.0 mmol) in dry ethanol (30 mL) was stirred at room temperature. After 48 h, all volatiles were removed under vacuum and the residue was dissolved in $CHCl_3$ (60 mL), washed with $H_2O$ (2 × 20 mL), and dried over $Na_2SO_4$. A brown solid was obtained after filtration and removal of the solvent was done under vacuum. The pure title compound was obtained as a light yellow solid (2.26 g, 69%) after column chromatography (silica: $CHCl_3$:MeOH = 1:9): mp 120 °C. $^1$H NMR ($CDCl_3$): $\delta$ 7.36 (1H, d, $^3J$ = 3.8 Hz), 7.28 (1H, d, $^3J$ = 3.6 Hz), 7.22 (1H, d, $^3J$ = 3.7 Hz), 7.15−7.19 (2H, m), 7.12 (1H, d, $^3J$ = 3.8 Hz), 7.06 (1H, dd). Anal. Calcd for $C_{17}H_{23}N_3O_2$: C, 67.75; H, 7.69; N, 13.94. Found: C, 68.01; H, 7.57; N, 13.82.

**Synthesis of 1-(*N*-Methylpyridinio)-2-[(*N*-methylpyrrol-2-yl)-5-methylene-diethanolamine]ethene Iodide (4).** A dry $CHCl_3$ (1 mL) solution of MeI (95 mg, 0.66 mmol) was added dropwise to a $CHCl_3$ (3 mL) solution of **2** (100 mg, 0.33 mmol). The reaction mixture was stirred overnight at room temperature. The resulting precipitate was collected and washed with a small quantity of $CHCl_3$. The bright orange solid was dried at 80 °C under vacuum and found to be the pure title compound **4** (140 mg, 95%): mp 168 °C. $^1$H NMR (DMSO-$d_6$): $\delta$ 8.57 (2H, d, $^3J$ = 6.6 Hz), 8.01 (2H, d), 7.85 (1H, d, $^3J$ = 15.8 Hz), 6.98 (1H, d), 6.79 (1H, d, $^3J$ = 3.6 Hz), 6.12 (1H, d), 4.32 (4H, t, $^3J$ = 5.2 Hz), 4.01 (3H, s), 3.72 (3H, s), 2.50 (4H, t). Anal. Calcd for $C_{18}H_{26}IN_3O_2$: C, 48.77; H, 5.91; N, 9.48. Found: C, 48.58; H, 5.77; N, 9.27.

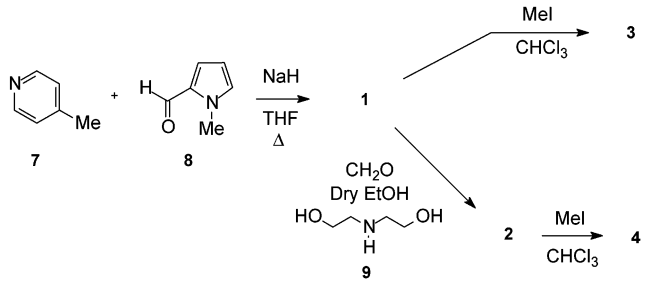


**Figure 4.** Synthesis of precursors **1** and **2** and the corresponding *N*-methylpyridinium salts **3** and **4**.

**Formation of Mono- and Multilayers.** (i) Coupling layer formation: Under $N_2$, freshly cleaned sodium lime glass was loaded into a Teflon sample holder and immersed in a dry toluene solution of *p*-(iodomethyl)phenyldiiodochlorosilane (**5**; 14 mM) for 30 min at room temperature. The colorless substrates were then washed twice with excess dry toluene and acetone and dried at 25 °C under vacuum. (ii) The functionalized substrates were spin-coated at 2000 rpm with a 20 mM solution of **1** or **2** in chloroform, covered with aluminum foil, and then heated at 105 °C in a vacuum oven (30 mmHg; static vacuum) for 20 min. The samples were cooled to room temperature under $N_2$ and then rinsed with excess chloroform and methanol to remove unreacted materials. Subsequently, the yellow substrates were dried at 105 °C under vacuum for 5 min and allowed to attain room temperature under vacuum. For preparation of multilayer **SAS-2**, (iii) capping with octachlorotrisiloxane (**6**): Under Ar, the dried substrates were immersed in a dry toluene solution of octachlorotrisiloxane (**6**; 34 mM) for 30 min, washed twice with dry pentane and acetone, and dried at 115 °C for 10 min. The substrates were cooled to 25 °C under vacuum before repeating steps (i)−(iii). Octachlorotrisiloxane (**6**) solutions were used for two repetitions. Solutions were filtered using Teflon-17F, 0.45-$\mu$m syringe filters (Osmonics, Inc.). Solvents were transferred using standard cannula techniques. Sonication was performed externally by immersing the glass reactor in a sonicator bath filled with water. Samples were handled and stored in the dark.

## Results and Discussion

**Synthesis of Pyrrole-Based Push−Pull/Donor−Acceptor Chromophores.** The new chromophore precursor **2** was prepared in simply two steps (Figure 4). Reaction of 4-picoline (**7**) with 1-methyl-2-pyrrolecarboxaldehyde (**8**) in the presence of NaH in THF afforded 1-(pyrid-4-yl)-2-(*N*-methylpyrrol-2-yl)ethene (**1**). The next step was envisioned considering that the electron-rich pyrrole ring[19] undergoes reaction with immonium electrophiles generated in situ from formaldehyde and a dialkylamine in the presence of an acid to afford the corresponding dialkylaminomethyl derivatives according to the Mannich protocol.[20] Since there is no appreciable charge transfer form the pyrrole to the pyridine rings in **1**,[15c] the pyrrole ring should be sufficiently electron-rich to react with the Mannich base. Indeed, a mixture of compound **1** with $(CH_2O)_n$ and diethanolamine (**9**) in the presence of *p*-toluenesulfonic acid in dry EtOH resulted in the formation of the new diethanolamino-

(13) Recently, SAS-based EO modulators were demonstrated: (a) Zhao, Y.-G.; Chang, S.; Wu, A.; Lu, H.-L.; Ho, S. T.; van der Boom, M. E.; Marks, T. J. *Opt. Eng. Lett.* **2003**, *42*, 298. (b) van der Boom, M. E.; Malinsky, J. E.; Zhao, Y.-G.; Chang, S.; Lu, W. K.; Ho, S. T.; Marks, T. J. *Polym. Prepr.* **2001**, *42*, 550−551. (c) Zhao, Y.-G.; Wu, A.; Lu, H.-L.; Chang, S.; Lu, W.-K.; Ho, S.-T.; van der Boom, M. E.; Marks, T. J. *Appl. Phys. Lett.* **2001**, *79*, 587−589. For a SA-based waveguiding SHG device, see: (d) Lundquist, P. M.; Lin, W.; Zhou, H.; Hahn, D. N.; Yitzchaik, S.; Marks, T. J.; Wong, G. K. *Appl. Phys. Lett.* **1997**, *70*, 1941−1943. For an ultrafast optical switch, see (e): Wang, G.; Zhu, P.; Marks, T. J.; Ketterson, J. B. *Appl. Phys. Lett.* **2002**, *81*, 2169−2171.

(14) For a recent report on siloxane-based zwitterionic monolayers as electro-optic materials, see ref 9.

(15) (a) Abbotto, A.; Beverina, L.; Bozio, R.; Facchetti, A.; Ferrante, C.; Pagani, G. A.; Pedron, D.; Signorini, R. *Org. Lett.* **2002**, *4*, 1495−1498. (b) Abbotto, A.; Beverina, L.; Bozio, R.; Bradamante, S.; Ferrante, C.; Pagani, G. A.; Signorini, R. *Adv. Mater.* **2000**, *12*, 1963−1967. (c) Bradamante, S.; Facchetti, A.; Pagani, G. A. *J. Phys. Org. Chem.* **1997**, *10*, 514−524. (d) He, G. S.; Yuan, L. X.; Prasad, P. N.; Abbotto, A.; Facchetti, A.; Pagani, G. A. *Opt. Commun.* **1997**, *140*, 49−52.

(16) (a) Facchetti, A.; van der Boom, M. E.; Abbotto, A.; Beverina, L.; Marks, T. J.; Pagani, G. A. *Polym. Prepr.* **2002**, *43*, 1292−1293. (b) Facchetti, A.; Abbotto, A.; Beverina, L.; van der Boom, M. E.; Marks, T. J.; Pagani, G. A. *Chem. Mater.* **2002**, *14*, 4996−5005.

(17) Malinsky, J. E.; Jabbour, G. E.; Shaheen, S. E.; Anderson, J. D.; Richter, A. G.; Marks, T. J.; Armstrong, N. R.; Kippelen, B.; Dutta, P.; Peyghambarian, N. *Adv. Mater.* **1999**, *11*, 227−231.

(18) Yitzchaik, S.; Roscoe, S. B.; Kakkar, A. K.; Allan, D. S.; Marks, T. J.; Xu, Z.; Zhang, T.; Lin, W.; Wong, G. K. *J. Phys. Chem.* **1993**, *97*, 6958−6960.

(19) Katritzky, A. R. *Handbook of Heterocyclic Chemistry*; Pergamon Press: Oxford, 1983.

(20) Joule, J. A.; Mills, K.; Smith, G. F. *Heterocyclic Chemistry*; Chapman & Hall: London, 1984.

**Table 1. Long-Wavelength UV−Vis Absorption Maxima ($\lambda_{max}$) of 1−4 and of the Self-assembled Chromophore Monolayers SA-1 and SA-2 on Glass**

| | $\lambda_{max}$ (nm) | | | | |
|---|---|---|---|---|---|
| compound | toluene | MeOH ($\epsilon$)[a] | $H_2O$ | film | $\Delta\lambda$[b] |
| **1** | 356[c] | 362 (21100)[c] | | | +6 |
| **2** | 363 | 366 (31000) | | | +3 |
| **3** | | 440 (39900) | 420 | | −20 |
| **4** | | 458 (38800) | 437 | | −21 |
| **SA-1** | | | | 448[c] | |
| **SA-2** | | | | 468 | |

[a] Extinction coefficient $\epsilon$ in l mol$^{-1}$ cm$^{-1}$. [b] $\Delta\lambda = \lambda_{max}$(solvent 1) − $\lambda_{max}$(solvent 2), with dielectric constants $\epsilon_1 > \epsilon_2$: positive $\Delta\lambda$ means positive solvatochromism. [c] From ref 15b.

**Table 2. Emission Data (Maximum of Fluorescence, $\lambda_f$, and Quantum Yield, $\Phi_f$)[a] of Dyes 3 and 4 in MeOH and DMSO**

| compound | solvent | $\lambda_{max}$ (nm) | $\lambda_f$ (nm)[b] | $\Delta\lambda$ (nm) | $\Phi_f$ | $E_g$ (eV)[c] |
|---|---|---|---|---|---|---|
| **3** | MeOH | 440 | 520 | 80 | 0.02 | 2.53 |
| | DMSO | 438 | 534 | 96 | 0.22 | 2.53 |
| **4** | MeOH | 458 | 533 | 75 | 0.02 | 2.47 |
| | DMSO | 454 | 549 | 95 | 0.13 | 2.44 |

[a] 9,10-Diphenylanthacene was used as standard ($\Phi_f = 0.90$ in cyclohexane). [b] Stokes shift. [c] Optical gap.

methyl-functionalized chromophore **2** in good yield. chiometric amount of methyl iodide in $CHCl_3$. The new diheteroarylethenes were thoroughly characterized using a combination of $^1$H NMR, UV−vis, and elemental analysis. Details are provided in the Experimental Section.

**Characterization of Chromophores in Solution.** Table 1 collects UV−vis data for **1**−**4** in different solvents and for the corresponding chromophore monolayers **SA-1** and **SA-2** (vide infra). As expected, salts **3** and **4** exhibit a bathochromic shift (78 and 92 nm, respectively) due to the alkylation at the azine nitrogen atom. The extent of these shifts is comparable since the push−pull core of **3** and **4** is identical for both systems. These salts have also similar solvatochromic responses ($\Delta\lambda \approx$ 20 nm), meaning that substitution at the 5-position of the pyrrole ring does not influence the molecular polarization.

The triflate salt of **3** is fluorescent when irradiated at the absorption maxima and was found to be an excellent two-photon lasing material, as reported elsewhere.[15d] Table 2 collects emission data in methanol and DMSO for chromophores **3** and **4**. Similarly, both systems emit in the visible region (520−550 nm) and exhibit similar fluorescence quantum efficiencies ($\Phi_f$ ). In general, $\Phi_f$ is found to be 1 order of magnitude larger in DMSO ($\Phi_f \sim 0.2$) than in MeOH ($\Phi_f \sim 0.02$). When the absorption and emission data are combined, the HOMO−LUMO (optical) energy gap can be estimated and is found to be ∼2.5 eV for both chromophores in solution.

Cyclic voltammetry measurements[21] on $\sim 10^{-3}$ M $CH_3CN$ solution of **2** and **4** (0.10 M $TBABF_4$ electrolite) show a chemically irreversible oxidative wave at +0.94 and +1.12 V, respectively. In addition, **4** exhibits a reductive wave at −1.2 V, indicating that alkylation of the nitrogen atom increases ionization potential and allows

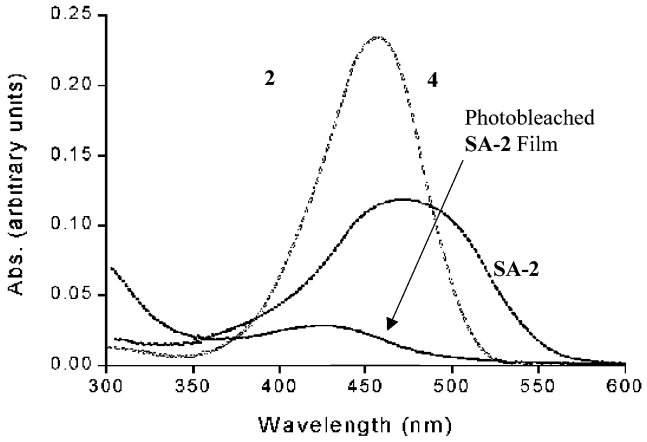


**Figure 5.** Transmission optical absorbance spectra (abs; arbitrary units). (i) Chromophore precursor **2** in methanol, (ii) chromophore **4** iodide salt in methanol, (iii) SA chromophore monolayer **SA-2** on a glass substrate, and (iv) the corresponding photobleached SA film.

electron injection. An estimated HOMO−LUMO gap[22] of ∼2.3 eV is found for **4** in very good agreement with the optical gap.

All of these data suggest that the intraoptical response of chromophores **3** and **4** is comparable. Therefore, it is expected that self-assembled mono- (**SA-2**) and multilayers (**SAS-2**) of **2** should preserve the good electro-optic response exhibited by **SA-1**,[16b] with the advantage of affording thicker films.

**Preparation and Characterization of Acentric Chromophore Monolayers.** Freshly cleaned float glass and Si(111) substrates were treated with a dry toluene solution of *p*-iodomethylphenyldiiodochlorosilane (**5**) at room temperature for 1 h under $N_2$ (Figure 3). The substrates were then washed with dry toluene and acetone and dried in vacuo. Subsequently, the colorless iodobenzyl-functionalized substrates were spin-coated with a layer of the chromophore precursor **2**, followed by vacuum oven treatment at 105 °C/30 mmHg for 20 min. The samples were then thoroughly rinsed with excess dry toluene and methanol to remove residual chromophore and then dried in vacuo at 105 °C for 5 min.

The resulting **2**-based monolayers were characterized by synchrotron X-ray specular reflectivity (XRR), angle-dependent polarized second-harmonic generation (SHG), optical (UV−vis) spectrometry, and advancing contact angle (CA) measurements. The new films strongly adhere to the hydrophilic substrates and cannot be removed by the "Scotch tape decohesion test"[23] and are insoluble in common organic solvents. Figure 5 shows the electronic spectra of **2** and **4** in methanol, a **2**-based SA film on glass, and a corresponding photobleached SA film. The monolayer formation on the glass substrates by selective quaternization of the pyridyl moiety with the covalently anchored benzyl iodide functionality is immediately obvious by the yellow color of the films. Indeed, the UV−visible spectra of **4** and of the corre-

(21) One-compartment cell with a Pt working electrode, Ag/0.1 M $AgNO_3$ ($CH_3CN$) reference, Ag counter electrode. The Ag/$AgNO_3$ reference electrode was additionally calibrated against ferrocene/ferrocinium ($E_{1/2} = 0.042$ V).

(22) Note that a precise determination requires knowledge of the standard potentials. Bard, A. J.; Faulkner, L. R. *Electrochemical Methods−Fundamentals and Applications*; Wiley: New York, 1984.

(23) (a) Nijmeijer, A.; Kruidhof, H.; Bredesen, R.; Verweij, H. *J. Am. Ceram. Soc.* **2001**, *84*, 136−140. (b) Krongelb, S. *Electrochem. Technol.* **1968**, *6*, 251−256.

sponding SA film (**SA-2**) exhibit a comparable red shift of the molecular charge-transfer band to $\lambda_{max} = 458$ nm (methanol) and $\lambda_{max} = 468$ nm (solid state), respectively, in comparison with the chromophore precursor **2** ($\lambda_{max} = 366$ nm; methanol). Importantly, no other features are observed, ruling out incorporation of chromophore precursor **2** into the film by alkylation of the trialkylamine group or formation of the types of molecular aggregates sometimes observed for LB films.[3,4] Thus, the chromophoric NLO unit is present as a pyridinium cation salt and the electroneutrality of the film is ensured by the external halide counteranion. The charge-transfer band of the SA film can be photobleached by illumination in air with visible light for a few days. After photodegradation, a new absorption band at $\lambda = 425$ nm is present. Photostimulated [2 + 2] cycloadditions at the ethene bridge in solution and in the solid state for similar push−pull conjugated compounds have considerable precedent.[15c] Similar conclusions were reached with **SA-1** films.[16b] Further evidence of chromophore monolayer formation is provided by advancing aqueous CA measurements, showing a decrease in $\theta_a$ from ∼68° for the substrates functionalized with a **5**-based coupling layer to ∼35° for the hydroxyl-group-terminated **SA-2** film. Monolayer **SA-1** was found to exhibit a slightly higher contact angle of ∼47°, in agreement with the absence of terminal OH groups.

XRR measurements were performed to gather detailed microstructural information on the **SA-2** films. In general, specular X-ray reflectivity is determined by the electron density profile $\rho(z)$ perpendicular to the sample surface. In the Born approximation, the normalized reflectivity is[24−26]

$$\frac{R(q_z)}{R_F(q_z)} = \left|\frac{1}{\rho_{Si}}\int \frac{\partial\rho(z)}{\partial z} e^{-izq_z}\, dz\right|^2 \qquad (1)$$

where the wave vector transfer $|\mathbf{q}| = q_z = (4\pi/\lambda)\sin\theta$ is along the surface normal, $\rho_{Si}$ is the electron density of the semi-infinite silicon substrate, $\rho(z)$ is the electron density distribution inside the film averaged over the in-plane coherence length of the X-rays (usually ∼1−3 $\mu$m), and $R_F(q_z)$ is the theoretical Fresnel reflectivity for an ideally flat substrate surface. For the present systems, a model consisting of a silicon substrate and layers of different electron densities, $\rho_i$, with Gaussian broadened interfaces, $\sigma_i$, was used,[24]

$$\frac{R(q_z)}{R_F(q_z)} = \left|\sum_{i=0}^{N}\frac{(\rho_i - \rho_{i+1})}{\rho_0} e^{-iq_zD_i} e^{-q_z^2\sigma_{i+1}^2/2}\right|^2 \qquad (2)$$

where $N$ is the number of layers, $\rho_0$ is the electron density of the substrate (=$\rho_{Si}$), $D_i = \sum_{j=1}^{i} T_j$ is the distance from the substrate surface to the $i$th interface, and $T_i$ is the thickness of the $i$th layer. The reflectivity data were fitted to such a model, the fitting parameters being the thickness of each layer, the electron density of each layer, and the root-mean-square width of each interface. It should be noted that eq 2 is valid for $q_z$ larger than approximately twice the critical wave vector for total external reflection ($q_c = 0.0316$ Å$^{-1}$ for silicon), where refraction effects are negligible. Thus, the fits were performed using only data for which $q_z > 2q_c$. Figure 6A shows normalized reflectivity data ($R/R_F$) from a typical scan on a **2**-based film. The corresponding

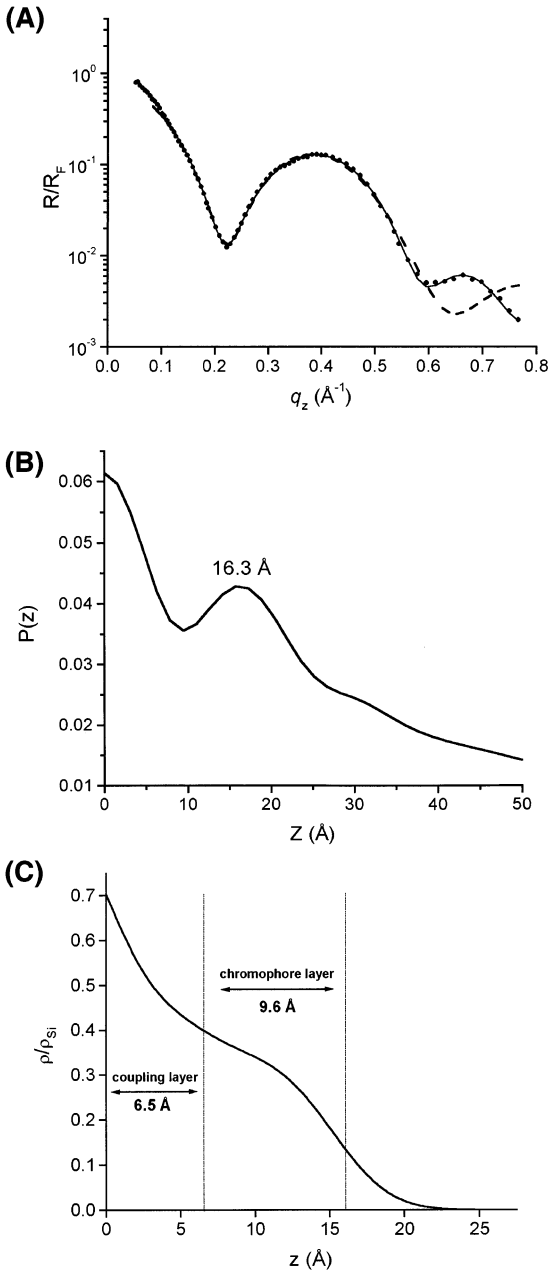


**Figure 6.** X-ray reflectivity data for films containing chemisorbed coupling agent (**5** in Figure 3) followed by chemisorption of chromophore precursor **2**. The structural model used for fitting the X-ray reflectivity data consists of a semi-infinite silicon substrate, a silicon oxide layer, a coupling layer, and a self-assembled chromophore layer. (A) X-ray reflectivity data normalized to the Fresnel reflectivity $R_F$. The dashed line is the fit to the data using a uniform electron density in the **2**-based film. The solid line is the best fit to the data using the two-region model described in the text. (B) Patterson function. (C) Plot of electron density ($\rho$) relative to silicon vs distance normal to the surface.

(24) (a) Als-Nielsen, J. *Physica A* **1986**, *140A*, 376−389. (b) Braslau, A. B.; Pershan, P. S.; Swislow, G.; Ocko, B. M.; Als-Nielsen, J. *Phys. Rev. A* **1988**, *38*, 2457.

(25) Tidswell, I. M.; Ocko, B. M.; Pershan, P. S.; Wasserman, S. R.; Whitesides, G. M.; Axe, J. D. *Phys. Rev. B* **1990**, *41*, 1111−1128.

(26) (a) *X-ray and Neutron Reflectivity: Principles and Applications*; Daillant, J., Gibaud, A., Eds.; Springer: Berlin, 1999. (b) Tolan, M. *X-ray Scattering from Soft-Matter Thin Films: Materials Science and Basic Research*; Springer Tracts in Modern Physics; Springer: Berlin, 1999; Vol. 148.

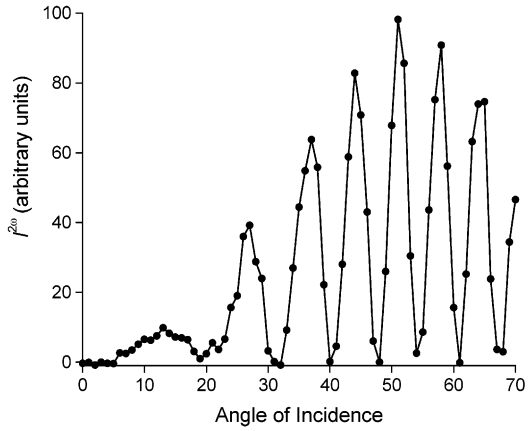


**Figure 7.** SHG response intensity ($I^{2\omega}$) as a function of fundamental beam incidence angle from a float glass slide having a **2**-based SA monolayer on either side.

one-dimensional Patterson functions calculated from XRR data are presented in Figure 6B. The large primary maximum is due to the substrate−film and film−air interfaces, and its position indicates that the overall thickness of the film is ∼16.3 Å. Figure 6C shows the best fit (dashed lines) using eq 2, assuming a uniform electron density in the film with error-function-broadened interfaces. The deviation from the experimental data is clear for $q_z > 0.5$ Å$^{-1}$. That means that the electron density within the film has a more complicated profile. However, assuming the presence of two different regions with different electron densities within the film, we have obtained a very good fit to the data (solid line in Figure 6A). The corresponding electron density distribution obtained from the XRR data is shown in Figure 6C. The first region, the coupling layer, has an electron density, $\rho_{coupling}$, of ∼0.33 e Å$^{-2}$, a thickness of ∼6.5 Å, and a "molecular footprint" of ∼47 Å$^2$. The second region, the chromophore layer, has a slightly lower electron density, $\rho_{chromophore}$, of ∼0.29 e Å$^{-2}$, a thickness of ∼9.6 Å, and a "molecular footprint" of ∼57 Å$^2$. Similar chromophore thickness and electron density values have been reported for related azobenzene and novel zwitterionic and heteroarylethene-based SA films.[9−11,16b] It therefore appears that ∼80% of the benzyl iodide functionalities of the coupling layer have undergone a reaction with **2**. The interfacial roughness, $\sigma_{coupling-chromophore}$, is only ∼2.4 Å and the surface roughness, $\sigma_{film-air}$, ∼3.1 Å, which is nearly identical to the Si(111) substrate roughness, $\sigma_{si-film}$, ∼2.6 Å. From the dye layer molecular footprint, the chromophore density ($N$s) can be calculated and is found to be ∼$1.8 \times 10^{14}$ molecules/cm$^2$. Similar observations were made with **SA-1**, which has a thickness of ∼15 Å and $N$s ∼ $2.1 \times 10^{14}$ molecules/cm$^2$.[16b]

Polarized angle-dependent SHG measurements on **SA-2** samples were made at $\lambda_o = 1064$ nm in the transmission mode. The characteristic SHG interference pattern from a glass substrate coated on both sides is shown in Figure 7, demonstrating that the quality and uniformity of the organic film is identical on both sides of the substrate. Related azobenzene-based monolayers with similar film thicknesses exhibiting large second-order macroscopic NLO responses, $\chi^{(2)} \sim 220$ pm/V and $r_{33} \sim 80$ pm/V, have 532-nm light-output responses ($I^{2\omega}$) comparable to the present **2**-based films. A $\chi^{(2)}$ value of

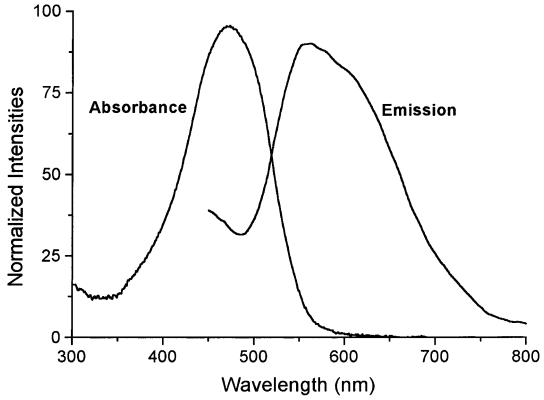


**Figure 8.** Transmission optical absorbance ($\lambda_{abs} = 470$ nm) and fluorescence ($\lambda_{em} = 560$ nm) of a film consisting of **2**-based trilayers.

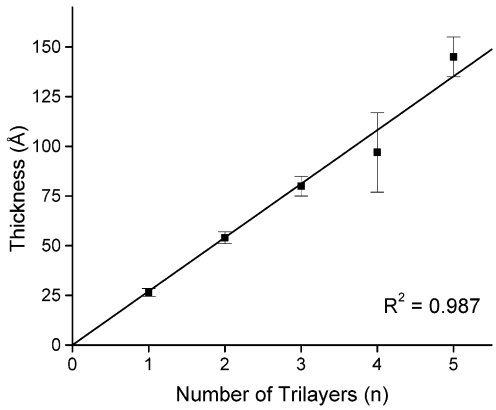


**Figure 9.** Linear dependence of the specular XRR-derived chromophoric superlattice thickness ($d$) vs number of **2**-based superlattice trilayers. An interlayer spacing of 33.8±1.3 Å is estimated.

∼120 pm/V was found for **SA-2**, which is slightly lower than that found for **SA-1** ($\chi^{(2)} \sim 142$ pm/V).[16b] Note that these new pyrrole-based films are completely transparent at the fundamental laser wavelength and, more importantly, only moderately absorbing at 532 nm (SHG light). Therefore, major $\chi^{(2)}$ enhancement due to overlap between the film CT absorption ($\lambda = 470$ nm) and the second-harmonic wave should be relatively small. It is known that such resonant effects can enhance experimental SAS film nonlinearities as much as 1 order of magnitude.[27]

**Formation and Characterization of Self-assembled 1-(Pyrid-4-yl)-2-(*N*-methylpyrrol-2-yl-5-methylenediethanolamine)ethene Multilayer Films.** The present three-step assembly methodology involves an iterative combination of (i) coupling layer deposition, (ii) spin-coating of **2** followed by a vacuum oven treatment, and (iii) capping of each chromophore layer with octachlorotrisiloxane (**8**, Figure 3). The iterative chemisorptive SA process and the resulting multilayer structural regularity have been characterized by UV−vis spectroscopy, advancing contact angle, XPS, XRR, AFM, and angle-dependent polarized SHG measurements.

Figure 8 shows typical one-photon absorption and emission spectra of a **2**-based multilayer. The linear

(27) Lundquist, P. M.; Yitzchaik, S.; Zhang, T.; Kanis, D. R.; Ratner, M. R.; Marks, T. J.; Wong, G. K. *Appl. Phys. Lett.* **1994**, *64*, 2194−2197.

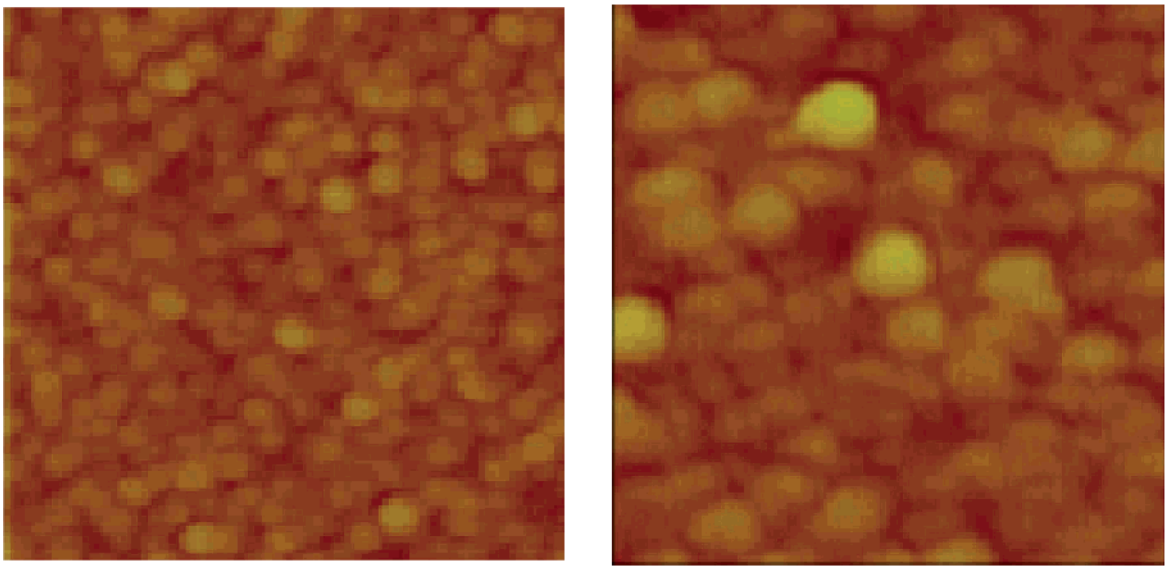

**A** **B**

**Figure 10.** AFM images at 1 × 1 $\mu$m scan areas of **SAS-2** composed of three (A) and five (B) trilayers.

absorption is centered around a maximum at $\lambda_{abs} = 470$ nm and the emission maximum is at approximately $\lambda_{em} = 560$ nm. Neither band shifts detectably upon multilayer formation, indicating homogeneous chromophore packing within the film. XPS measurements reveal the presence of Si, C, O, N, I, and Cl. The inclusion of Cl in the films is probably caused by an anion exchange process. Upon capping layer, $-SiO_x-$ deposition, the chromophore salt may undergo $Cl^-/I^-$ exchange with traces of HCl. Previous studies showed that chloride counteranions with SA monolayers can undergo ion exchange with various anions (e.g., iodide, sufanilate, ethylorange, and eosin).[28] Aqueous CA measurements reveal the formation of a hydrophilic surface, $\theta^a \sim 20°$, after capping layer deposition (step iii).

The linear dependence of the XRR-derived film thickness on the number of assembled coupling/chromophore/capping trilayers indicates the buildup of microstructurally uniform films up to 15 layers (Figure 9). However, thicker films are conceivable. Organic SAS films exhibiting good structural regularity up to 80 layers were recently demonstrated by us.[10i] From the slope of the XRR measurements, an average inter(tri)layer spacing of 33.8 ± 1.3 Å can be estimated, very close to ~32 Å found in the above-mentioned azobenzene-base superlattices.[10i]

Contact mode AFM measurements were performed on each of five trilayer samples, from one to five trilayers. This study reveals an increased grain texture and an RMS surface roughness going from 0.3 to 2.1 nm, respectively, for 1 × 1 $\mu m^2$ scan areas (Figure 10). Grain formation is a common phenomenon in layer-by-layer assemblies.[7,8] Scanning force microscopy studies of organic−inorganic hybrid films prepared with group 13 oxide interlayers and group IV metal-coordination-based SASs reveal also grain-type topographies and surface roughnesses.[7,8] However, more studies are required to elucidate the origin of this process.

(28) Roscoe, S. B.; Yitzchaik, S.; Kakkar, A.; Marks, T. J. *Langmuir* **1996**, *12*, 5338−5349.

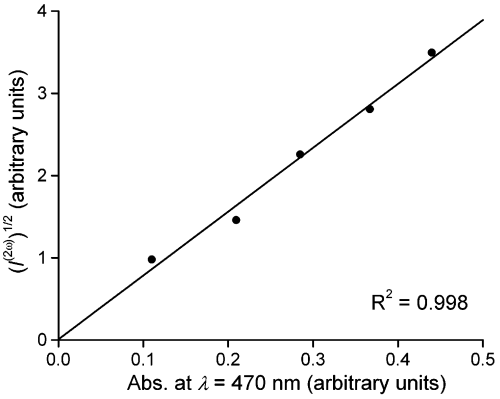


**Figure 11.** Linear dependence with the number of **2**-based trilayers of the square root of the SH intensity ($I^{2\omega}$) as a function of absorption at $\lambda_{max} = 470$ nm. The incident angle of the fundamental beam was 50°.

Finally, for a microstructurally regular polar multilayer, with minimal self-absorption, the SHG intensity ($I^{2\omega}$) is expected to scale quadratically with the number of chromophore deposition cycles[27] because the incident light wavelength (1.06 $\mu$m) is large compared to the SA film thickness. Indeed, the observed linear dependence and zero intercept of $(I^{2\omega})^{1/2}$ vs the HOMO−LUMO CT absorbance at $\lambda = 470$ nm on the number of trilayers (Figure 11) demonstrates that approximately equal densities of uniformly polar-oriented chromophores are deposited in each assembled trilayer while maintaining good structural regularity.

## Conclusions

We have shown here that new $\pi$-deficient pyridinium−(C=C)−$\pi$-excessive pyrrole-based chromophores can be successfully integrated into highly transparent, structurally regular, and acentric SAS multilayer films. Our results indicate that the known three-step assembly method is suitable for a wide range of push−pull/donor−acceptor chromophores.[11a,b]

The possibility to prepare microstructurally regular multilayers exhibiting good electro-optic response is a

prerequisite for their possible practical applications. We are aware that the films reported here are still too thin for micrometer-size device fabrication. However, various prototypes of frequency doubling devices, frequency-selective, ultrafast optical switches, and electro-optic modulators have been demonstrated by us recently, employing similar sub-micrometer-thick multilayer assemblies.[29] Efforts toward the fabrication of thicker films are in progress and will be reported in future contributions.

Finally, the use of high-$\beta$ chromophores based on other five-membered monoheterocycles (e.g., thiophene, furan, and benzo-fused systems)[14c] with relative $\pi$-excessive/deficient natures, as established by $\sigma_r$ values and oxidation potentials,[30] should allow further fine-tuning of superlattice physicochemical properties (e.g., $\lambda$, $\chi^{(2)}$, $r_{33}$) and eventually enhance material performance.[13]

**Acknowledgment.** Research supported by the NSF MRSEC program (Grant DMR0076077 to the Northwestern Materials Research Center), by ARO/DARPA (DAAD19-00-1-0368), by MIUR (Grant 2001034442), and by CNR-Progetto Finalizzato Materiali Avanzati II. Part of this work was perfomed at beamline X23B of the National Synchrotron Light Source, which is supported by the U.S. Department of Energy. We also thank Mr. P. A. Lee and Prof N. R. Armstrong (U. of Arizona) for XPS measurements.

CM020929D

(29) For more discussion of multilayer film-based devices see ref 10 (i) and Ma, H.; Jen, A. K.-Y.; Dalton, L. R. *Adv. Mater.* **2002**, *14*, 1339−1365.

(30) (a) Zotti, G.; Shiavou, G.; Berlin, A.; Pagani, G. *Synth. Met.* **1991**, *40*, 299. (b) Zotti, G.; Shiavon, G.; Comisso, N.; Berlin, A.; Pagani, G. *Makromol. Chem.* **1990**, *36*, 337. (c) Charton, M. *Prog. Phys. Org. Chem.* **1981**, *3*, 119.